Probe diagnostics of non-Maxwellian plasmas

V. A. Godyak, R. B. Piejak, and B. M. Alexandrovich
Osram Sylvania Inc., 100 Endicott Street, Danvers, Massachusetts 01923

(Received 21 September 1992; accepted for publication 21 December 1992)

Various probe diagnostic methods have been applied to rf plasmas with non-Maxwellian electron energy distribution functions (EEDF) and the results of these diagnostic methods have been compared. Plasma density and electron temperature were obtained using standard procedures from the electron retardation region (classic Langmuir method), the ion saturation region, and the electron saturation region of the measured probe I/V characteristic. Measurements were made in a 13.56-MHz capacitive argon rf discharge at two gas pressures: $p=0.03$ Torr, where stochastic electron heating is dominant, and $p=0.3$ Torr, where collisional electron heating dominates. Thus, the measured EEDF at each gas pressure manifests a distinct departure from thermodynamic equilibrium being bi-Maxwellian at 0.03 Torr and Druyvesteyn-like at 0.3 Torr. Considerable differences in electron density and temperature were obtained from the different parts of the probe characteristic and these values differ dramatically in many cases from those found from integration of the measured EEDF's, thus demonstrating that using standard procedures in non-Maxwellian plasma can give misleading results.

I. INTRODUCTION

Electrostatic probes are indispensable diagnostic tools in low-pressure weakly ionized plasmas. The ability to locally measure various plasma parameters over a wide range of experimental conditions and to measure the electron energy spectrum makes probe methods superior in many instances to other plasma diagnostic techniques. The main application of probe methods is in the area of low-pressure electrical gas discharges where strongly nonequilibrium plasmas are typically encountered. Electrons in such plasmas are not in energy equilibrium with ions or neutrals, having an electron temperature T_e which is usually much greater than the ion or neutral temperatures, T_i and T_g, respectively. Moreover, although widely used conventional probe theories for electron and ion currents assume a Maxwellian EEDF, the electron energy distribution function, $F(\epsilon)$, in low-pressure discharges is generally non-Maxwellian and the electron temperature is usually thought of as an effective electron temperature T_{eff} corresponding to a mean electron energy $\langle\epsilon\rangle$ determined from the EEDF.

In practice one usually neglects non-Maxwellian effects in inferring plasma parameters from the probe characteristics assuming that a departure of the actual EEDF from Maxwellian only affects a small number of electrons with energies higher than the energy of the inelastic threshold ϵ^*. Unfortunately, in many cases the EEDF in low-pressure discharges is not Maxwellian even in the low-energy range where $\epsilon<\epsilon^*$ and application of conventional procedures for processing probe characteristics in non-Maxwellian plasmas may lead to significant errors in the determination of basic plasma parameters.

The purpose of this work is to compare plasma parameters determined from the measured probe characteristic using various well known analysis techniques in a discharge where the electron energy spectrum is non-Maxwellian. The effective electron temperature T_{eff}, plasma density n, and plasma space potential V_s have been obtained from the measured probe I-V characteristics $I_p(V)$ using the following techniques:

(a) Druyvesteyn procedure: differentiating the probe characteristic to obtain the EEDF and determining T_{eff} and n as corresponding integrals of the EEDF. The plasma potential found here is the zero crossing point of the second derivative of the probe current.

(b) Classical Langmuir procedure applied to the electron retardation region of the probe characteristics corresponding to electron collection when the probe potential V is less than the plasma potential.

(c) Orbital motion limit (OML) theory[3,4] for electron collection in the electron saturation region of the probe characteristic ($V>V_s$).

(d) OML theory for ion collection in the ion saturation region of the probe characteristic.[3,5]

(e) Radial motion theories of ion collection.[13–15]

II. EEDF MEASUREMENTS

The probe measurements presented here have been performed on the axis of the mid plane of a symmetrically driven capacitively coupled rf discharge in argon at 13.56 MHz. A detailed description of the experimental setup and measurement procedures is given in Ref. 1. Measurements were made at a discharge current density of 1 mA/cm^2 for two different gas pressures: $p=0.3$ and $p=0.03$ Torr. These gas pressure were specifically chosen to provide discharge regimes where the electron heating processes that sustain the discharge are distinctly different.[2] At $p=0.3$ Torr the discharge is collision dominated while at $p=0.03$ Torr the discharge is sustained mainly through stochastic heating. As shown in Fig. 1, the different discharge sustaining processes result in essentially different shapes in the electron energy probability function (EEPF), $f(\epsilon)=\epsilon^{-1/2}F(\epsilon)$, which would be a straight line for a Max-

 0021-8979/93/083657-07$06.00

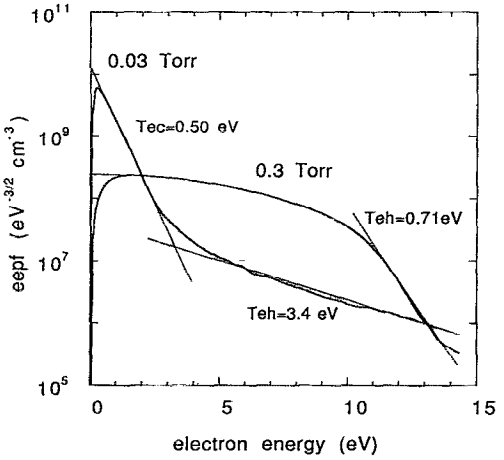

FIG. 1. The EEPF measured in an argon capacitive rf discharge at 13.56 MHz for $p=0.03$ and 0.3 Torr.

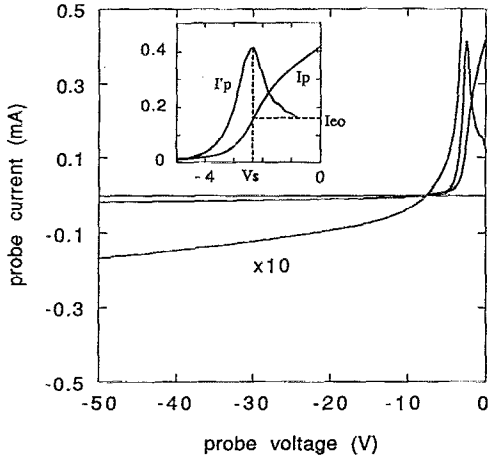

FIG. 2. Probe I-V characteristic: I_p and its first derivative I_p' for $p=0.03$ Torr. The plasma potential V_s and the electron saturation current I_{e0} correspond to the maximum of I_p'.

wellian EEPF in this representation. The EEPF's shown in Fig. 1 were obtained from the Druyvesteyn formula

$$f(\epsilon)=2(2m_e)^{1/2}(e^3A)^{-1}\,d^2I_p/dV^2,$$

where e and m_e are the electron charge and mass, V and I_p are the probe voltage and current, and A is the probe surface area.

The EEPF at 0.03 Torr can be represented as a bi-Maxwellian with a cold-electron group having temperature $T_{ec}=0.50$ eV and density $n_c=4.2\times10^9$ cm^{-3} and a hot-electron group having $T_{eh}=3.4$ eV and $n_h=2.4\times10^8$ cm^{-3}. Note that the departure from a Maxwellian distribution starts at $\epsilon\approx3$ eV, which is much less than the excitation energy ϵ^* for argon (11.55 eV). Integration of the EEDF at 0.03 Torr gives

$$n=\int_0^\infty F(\epsilon)d\epsilon=4.4\times10^9\ \text{cm}^{-3}$$

and

$$T_{\text{eff}}=\frac{2}{3}\langle\epsilon\rangle=2(3n)^{-1}\int_0^\infty \epsilon F(\epsilon)d\epsilon=0.67\ \text{eV}.$$

The EEPF at 0.3 Torr is Druyvesteyn-like: $f(\epsilon)\propto\exp-(\epsilon^2/\alpha^2)$ in the energy interval up to ϵ^* (where α is a constant related to the energy gained from the field over an electron mean free path length) and then linearly drops for $\epsilon>\epsilon^*$ with a hot-electron distribution "temperature" $T_{eh}=0.71$ eV. Integration of the EEDF at 0.3 Torr gives $n=2.9\times10^9$ cm^{-3} and $T_{\text{eff}}=3.4$ eV.

In what follows the plasma parameters obtained from EEDF measurements are considered as a reference to which plasma parameters obtained using conventional procedures, based on assuming a Maxwellian EEDF, will be compared.

III. LANGMUIR PROCEDURE

The full I/V characteristics measured by the probe are shown in Figs. 2 and 3 for 0.03 Torr and 0.3 Torr, respectively. The first derivative $I_p'(V)$ is also shown in each figure and the plasma potential (the probe voltage where I_p' is maximum) is identified. Finding the plasma potential by differentiating the probe characteristic is more definitive and accurate than finding it from a semilog plot of the electron current versus the probe potential. In Fig. 4, probe characteristics are given in semilog scale and plasma potential, determined from the maximum of I_p', is indicated by a horizontal arrow. For 0.03 Torr the plasma potential corresponds to an inflection point rather than the crossing point between extrapolated lines of the probe characteristic. (Extrapolating lines tangent to the probe characteristic to identify the crossing point is a procedure recommended in some texts to find plasma potential.) Similar to the EEPF the probe characteristic for 0.03 Torr also demonstrates a two-electron temperature structure with $T_c=0.73$ and $T_h=4.2$ eV. Although these temperatures differ somewhat from those found from the EEPF shown in Fig. 1,

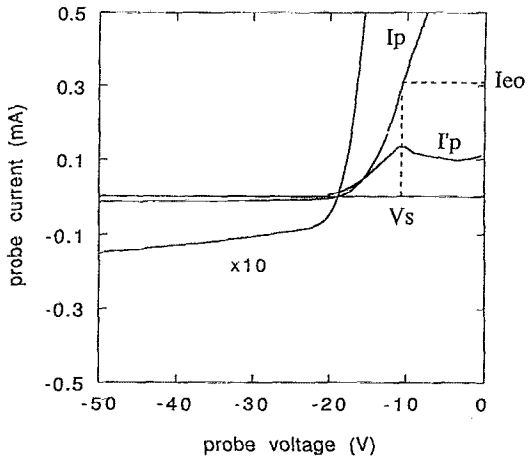

FIG. 3. Probe I-V characteristic: I_p and its first derivative I_p' for $p=0.3$ Torr. The plasma potential V_s and the electron saturation current I_{e0} correspond to the maximum of I_p'.

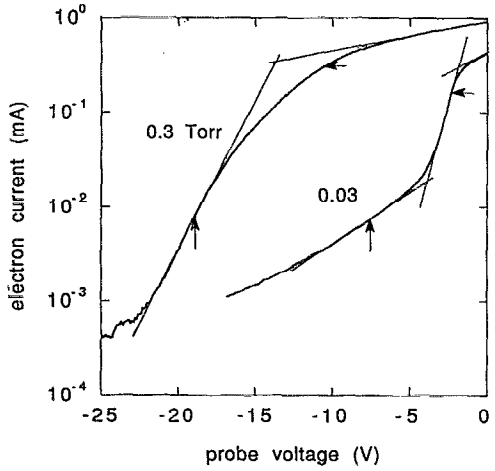

FIG. 4. The electron current to the probe in semilog scale. The horizontal arrows show the plasma potential and the vertical arrows show the floating potential.

this difference seems reasonable since in general I_e is not proportional to its second derivative and only for a Maxwellian (exponential) EEPF is $I_e \propto I_e''$.

The plasma density may be obtained from the Langmuir formula

$$I(V_s)=eAn(T_e/2\pi m_e)^{1/2}.$$

For $I_e(V_s)$ and $T_e=T_c$, $n_L=3.3\times10^9$ cm^{-3} while the density found from the $I_e(V_s)$ at the crossing point of the extrapolated curves is $n_{cr}=5.9\times10^9$ cm^{-3}. In a corresponding way, using T_{eff} gives $n_L^0=3.5\times10^9$ cm^{-3} and $n_{cr}^0=6.2\times10^9$ cm^{-3}. All these values are close to the true value $n=4.4\times10^9$ cm^{-3} found through integration of the EEDF.

The semilog plot of $I_e(V)$ for 0.3 Torr is a bit puzzling since there is no sign of a break in this curve at the plasma potential where $I_p'(V)$ is at a maximum. Following the standard prescription for processing the probe characteristic, two linear parts of the function ln $I_e(V)$ are extrapolated to their crossing point to determine the plasma potential giving a plasma potential which is 3 V lower than the true plasma potential designated in Fig. 4 by a horizontal arrow. The linear part of this curve, which appears around the floating potential (shown by the vertical arrow), gives an "electron temperature" of 1.37 eV and corresponding values of n_L and n_{cr} are 4.5×10^9 cm^{-3} and 5.2×10^9 cm^{-3}. If one uses the value of T_{eff} found from integrating the EEDF the corresponding values for n_L^0 and n_{cr}^0 are 2.9×10^9 cm^{-3} and 3.3×10^9 cm^{-3}. The standard procedure for determining the electron temperature gives a value 2.5 times less than T_{eff} found from the EEDF while the values of plasma density are not too far from those found from the EEDF. In the cases of 0.03 Torr and 0.3 Torr, the plasma density n_L^0 found from electron saturation current $I_e(V_s)$ matches the true plasma density better than if one uses the plasma potential and effective electron temperature found through differentiation of the probe characteristic.

It is interesting to note that essentially different numbers for the normalized floating potential $\eta_f^0=e\Delta V_f/T_{\text{eff}}$ follow from the probe characteristics, where ΔV_f is the probe floating potential referenced to the plasma potential $\Delta V_f=V_s-V_f$, thus, $\eta_f^0=7.8$ for $p=0.03$ Torr and $\eta_f^0=2.4$ for $p=0.3$ Torr. Under the present experimental conditions with the probe radius $a=6.35\times10^{-3}$ cm being close to the Debye length λ_D, for a Maxwellian EEDF one should expect η_f in both cases to be

$$\eta_f=1/2\ln[b^2/a^2(m_i/3.6m_e)]\approx4,$$

where b is the ion collection sheath radius, and m_i and m_e are the electron and ion mass, respectively. The differences between the experimentally measured values of η_f^0 and those derived here for the Maxwellian EEDF are due to the shape of the high-energy part of the measured EEDF since a floating probe only collects those electrons with energies higher than the energy barrier created by the floating potential.

IV. USING OML THEORY FOR THE COLLECTION OF ELECTRONS

OML theory was introduced by Langmuir and Mott-Smith[3] and can be used to calculate the probe current of attracted (accelerated) particles. This theory implies a thick, collisionless sheath ($\lambda_{e,i}\gg b\gg a$), where $\lambda_{e,i}$ is the electron or ion mean free path. Assuming a Maxwellian energy distribution in the unperturbed plasma, the following simplified formula for a cylindrical probe may be used to determine the electron current in the OML regime:[7]

$$I_{e,i}=2/\sqrt{\pi}Aen(T_{e,i}/2\pi m_{e,i})^{1/2}(eV_p/T_{e,i}+1)^{1/2}$$
$$\approx\sqrt{2}/\pi Aen(|eV_p|/m_{e,i})^{1/2}.$$

Applied to the electron current, this formula has been successfully used by many authors. Good agreement with the classic Langmuir procedure for inferred plasma density has been demonstrated by Verweij[4] for gas pressures up to 20 Torr and plasma density up to 10^{12} cm^{-3} using a very thin ($a=1\times10^{-3}$ cm) cylindrical probe. Since normally $\lambda_e\gg\lambda_i$, apparently the limit of applicability on OML theory is not as strict for electron collection as it is for ion collection.

The calculation of Laframboise[5] based on the more complete theory of Bernstein and Rabinowitz[6] showed that the OML limit is achieved for $\lambda_D\approx a$. The Debye lengths calculated using values of n and T_{eff} found from the measured EEDF for 0.03 and 0.3 Torr are 9.1×10^{-3} cm and 2.5×10^{-2} cm, respectively, while corresponding electron free paths are 8.3 cm and 0.095 cm. Thus the requirements for applicability of the OML theory are satisfied for the probe radius ($a=6.35\times10^{-3}$ cm) used in this experiment.

The square of the electron current $I_e^2(V_p)$ versus probe voltage ($V_p=V-V_s$) for two gas pressures is plotted in Fig. 5 along with the linear extrapolation of each curve back to the abscissa. In accordance with OML theory the slope of the linear extrapolation yields the plasma density without knowledge of the electron temperature. Values of plasma density for 0.03 and 0.3 Torr are nOMLe = 3.7

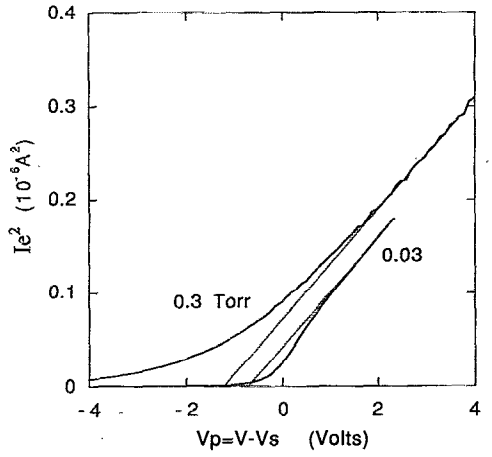

FIG. 5. The electron probe current squared vs probe voltage for $p=0.03$ and 0.3 Torr.

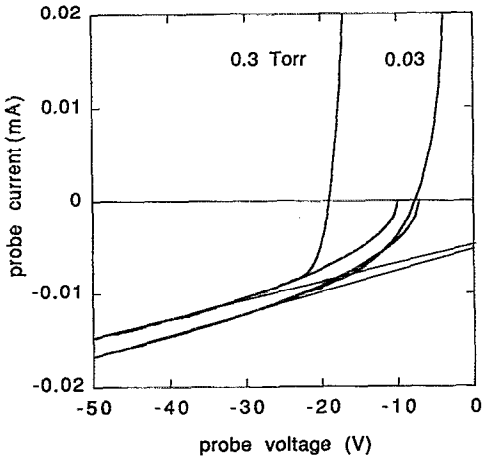

FIG. 6. Linear and parabolic approximations of the ion currents.

$\times 10^9$ cm^{-3} and 3.6×10^9 cm^{-3}, respectively, which are in good agreement with those values obtained from the EEDF. OML theory also allows one to find the electron temperature from the difference between the plasma potential and the crossing point on the voltage axis of the extrapolated $I_e^2(V)$ line but this can only be done if the plasma potential is known beforehand from an independent measurement. The electron temperature found in this way is 0.65 eV for 0.03 Torr, which agrees very well with T_{eff}, while for 0.3 Torr it is 1.23 eV, almost three times less than T_{eff}. Note that generally the function $I_e^2(V)$ changes slope with probe voltage and therefore n_e and T_e obtained using this procedure are quite subjective and largely dependent on the range of the probe characteristic, thus suffering from a rather large degree of uncertainty.

V. USING ION PART OF THE PROBE CHARACTERISTIC

The ion part of the probe characteristic is frequently used in plasma diagnostics. In this method the electron temperature is found from the slope of the probe characteristics near the floating potential V_f. For a single probe the electron temperature may be written as

$$T_e^i = eI_{if}(dI_e/dV)^{-1}$$

$$= eI_{if}(dI_p/dV - dI_i/dV)^{-1} \quad \text{evaluated at } V=V_f,$$

where I_{if} is an extrapolation of the ion current to the probe. Extrapolation of the ion current towards the plasma potential is somewhat arbitrary and could result in misleading conclusions. Two commonly used extrapolation techniques, linear and parabolic, are shown in Fig. 6. For 0.3 Torr, the parabolic approximation crosses the zero current line near the plasma potential. For 0.03 Torr, the crossing takes place near the floating potential. The latter suggests an absence of electron current at a probe potential lower than the floating potential corresponding to an EEDF which is severely depleted of high-energy electrons. In fact, for 0.03 Torr, the measured EEDF demonstrates an excessive number of high-energy electrons. This example shows how misleading a parabolic approximation of ion current can be in the evaluation of the electron current for $V<V_f$ and in finding the plasma potential.

Since at the floating potential the probe is accessible only to electrons having an energy larger than $e|V_f-V_s|$ the electron temperature obtained from the slope of the probes I-V characteristic at the floating potential, V_f, is governed by the high-energy part of the EEDF and thus is valid only for an EEDF which is Maxwellian over a very large energy range. Note that in a majority of cases for low-pressure gas discharges, a departure from Maxwellian-like EEDF takes place at energy less than $e|V_f-V_s|$.

Using a linear extrapolation of the probe ion currents, as shown in Fig. 6, the electron temperature T_e^i found from the ion part of the probe characteristics are 3.6 eV for 0.03 Torr and 1.4 eV for 0.3 Torr, which are in dramatic contradiction to the corresponding values of T_{eff} (0.67 eV and 3.4 eV, respectively) found from the EEDF's. Ironically, these errors in T_e^i and their trend with gas pressure are in general agreement with elementary theory of gas discharge plasmas assuming a Maxwellian EEDF (see Von Engel,[8] for example).

Calculation of the plasma density from the ion current can be carried out in a number of ways. The most popular approach, introduced by Langmuir, is to use OML theory. OML theory is widely used for two reasons: first, when applicable it is easy to use since it does not require knowledge of the electron temperature, and plasma potential and second, in many experiments I_i^2 is found to be a linear function of the probe voltage and this behavior is expected when OML theory applies. Unfortunately, as Langmuir and many others have pointed out, this is not a sufficient condition to ensure validity of OML theory. As shown in Fig. 7 the values of I_p^2 versus probe voltage are linearly related at large negative probe voltages where $|I_e| \ll |I_i|$. The plasma density predicted using OML theory for 0.03 and 0.3 Torr are 1.1×10^{10} and 9.6×10^9 cm^{-3}, respectively, and these values of plasma density differ by only 2% from those calculated with Laframboise theory. For the

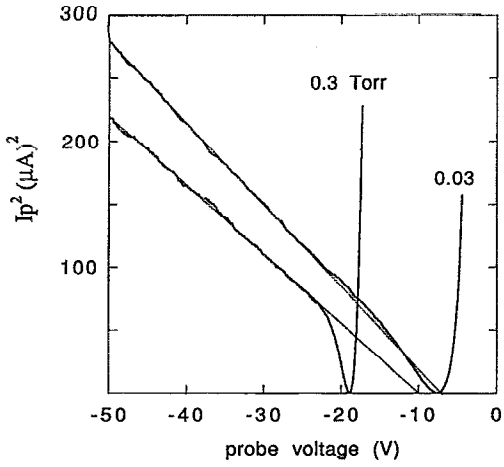

FIG. 7. The ion probe current squared vs probe voltage for $p=0.03$ and 0.3 Torr.

probe radius and Debye length in this experiment the Laframboise and OML theories actually coincide. For either derivation the density appears to be 2–3 times larger than the actual values determined from the EEDF's.

Exaggerated values for plasma density obtained from ion current using OML theory were noted by Langmuir and Smith and Plumb[9] and also in more detailed studies of Sonin[10] and Shih and Levi.[11] It has been shown (see Ref. 11 and literature therein) that ion-ion and ion-atom collisions as well as the finite length of the cylindrical probe significantly affect ion orbital motion and tend to destroy it. As a result, the ion current to the probe under such conditions corresponds to radial ion motion rather than to orbital motion. This has been shown in experiments.[10,12] Shih and Levi showed that the OML regime for a cylindrical probe is destroyed when $\lambda_i/a<(eV_p/T_i)^{1/2}\gg 1$, where $\lambda_i^{-1}=\lambda_{in}^{-1}+\lambda_{ii}^{-1}$ and represents the ion mean free path accounting for both ion-neutral (in) and ion-ion (ii) collisions. Since V_p is usually tens of volts and T_i is close to room temperature and is tens of millivolts, the OML regime is already destroyed at very low gas pressures (in our experiment with $a=6.35\times 10^{-3}$ cm at $p>0.02$ Torr).

The unsuitability of OML theory for inferring plasma density from the ion current inevitably complicates the analysis. One difficulty is that alternatives, such as, the radial motion theories of Allen, Boyd, and Reynolds[13] presented by Chen[14] for cylindrical probes (ABRC theory), as well as Laframboise calculations[5] are difficult to use in practice since they are given graphically by sets of normalized ion current/voltage characteristics for discrete values of a/λ_D which depend on plasma density. This procedure can be done more easily using Sonins normalization requiring only one universal curve. Also these theories require knowledge of the probe sheath voltage V_p, which is found from the measured floating potential assuming a Maxwellian EEDF as follows:

$$V_p=V-V_f-T_e/2e\ln(b^2m_i/a^2m_e).$$

Since the effective ion collection radius b is unknown *a priori*, inference of the plasma density from the measured ion current and the floating potential requires a cumbersome iteration procedure. This is why these theories are used mostly in confirmatory mode[12] (confirming parameters found in advance using another technique) rather than in a predictive mode.

Additional problems arise for non-Maxwellian EEDF when T_e^i found from the ion part of the probe characteristics does not correspond to the mean electron energy or T_{eff}. Under such conditions the use of T_e^i leads to an error in evaluating the probe sheath voltage V_p and to an error in calculating the normalized ion current J_i in the ABRC theory:

$$I_i=J_i(-eV_p/T_e,a/\lambda_D)[A\epsilon_0/ea^2(2T_e^3/m_i)^{1/2}],$$

where ϵ_0 is the vacuum permittivity.

Knowing the Debye length from EEDF measurements for 0.03 Torr we have evaluated J_i (using Chen's curves) and found the values of the ion current I_i for $\eta=-eV_p/T_e=20$ at two values of electron temperature T_e^i and T_{eff}. It appears that $I_i(T_e^i)$ is eight times larger than corresponding experimental values while $I_i(T_{\text{eff}})$ is larger by only 60%. At 0.3 Torr the probe sheath appeared to be collision dominated ($\lambda_i\ll b$) and ABRC theory is not applicable. Nonetheless, the use of two electron temperatures T_e^i and T_{eff} gives corresponding theoretical values for I_i that are 40% smaller and 80% larger than the measured I_i.

For evaluation of the plasma density when the ion current is controlled by radial motion we used an approach introduced by Kagan and Perel[15] (KP) which is more convenient to use than the previous theories. With this approach there is no need to iterate to find the plasma density but uncertainty in the probe sheath voltage V_p still remains for a non-Maxwellian EEDF. In this approach ion current to the probe is considered as space-charge-limited current given by the Child–Langmuir Law for a cylindrical geometry:

$$I_i=\tfrac{4}{9}\epsilon_0(2e/m_i)^{1/2}AV_p^{3/2}/a^2(-\beta^2),$$

where $(-\beta^2)$ is a tabulated function of b/a. The ion current is governed by the collecting surface which is b/a times larger than the probe surface A, such that

$$I_i=0.4(b/a)Aen(2T_e/m_i)^{1/2}.$$

In using this approach one finds $(-\beta^2)$ from CL Law and after determining b/a the plasma density can readily be found from the ion current (second) equation. Again, the departure from a Maxwellian EEDF or differences in T_{eff} and T_e^i affect the inferred value of plasma density. This comes about in two ways, through the dependence of $(-\beta^2)$ and b from V_p in the CL Law and via the dependence $I_i\propto bT_e^{1/2}$ in the ion current equation. Evaluation of b/a for both pressures and $|V_p|=30$ V gives $b/a=13$, which corresponds to a $b/\lambda_i=0.58$ for 0.03 Torr and $b/\lambda_i=5.8$ for 0.3 Torr. Apparently, in the second case the probe sheath is in a collision-dominated regime and neither ABRC nor KP theory is applicable. The plasma density n_{KP}^i calculated using the electron temperature obtained from the ion part of the probe characteristic (T_e^i for 0.03

TABLE I. Plasma parameters inferred using various procedures.

Parameter	p=0.03 Torr	p=0.3 Torr	Notes
n (cm^{-3})	4.4×10^{9}	$2.9\cdot10^{9}$	$\lambda_e\approx$8.3 cm, p=0.03 Torr; 0.95 cm, p=0.3 Torr
T_{eff} (eV)	0.67	3.4	$\lambda_i=1.4\times10^{-1}$ and 1.4×10^{-2} cm
λ_D (cm)	9.1×10^{-3}	$2.5\cdot10^{-2}$	$a=6.35\times10^{-3}$ cm
n_c (cm^{-3})	4.2×10^{9}	...	λ_e is estimated from argon cross section at $\epsilon=3/2\ T_{\text{eff}}$.
T_{ec} (eV)	0.50	...	λ_i found from charge-exchange cross section.
n_h (cm^{-3})	2.4×10^{8}	...	
T_{eh} (eV)	3.4	(0.71)	T_{eh} for p=0.3 Torr is the decay parameter of EEPF for high-energy electrons.
		(a) Druyvesteyn procedure (from EEDF)	
n_L (cm^{-3})	3.3×10^{9}	4.5×10^{9}	The plasma potential was found through differentiation of the probe characteristics.
T_{eL} (eV)	0.73	1.37	
T_c (eV)	0.73	?	
T_h (eV)	4.2	1.37	
n_{cr} (cm^{-3})	$5.9\cdot10^{9}$	$5.2\cdot10^{9}$	
n_L^0 (cm^{-3})	$3.5\cdot10^{9}$	$2.9\cdot10^{9}$	These values were found using T_{eff} from EEDF.
n_{cr}^0 (cm^{-3})	$6.2\cdot10^{9}$	$3.3\cdot10^{9}$	
η_f^0	7.8	2.4	
		(b) Langmuir procedure [from ln, $I_c(V)$]	
n_{OML}^e (cm^{-3})	3.7×10^{9}	3.6×10^{9}	
T_{OML}^e (eV)	0.65	1.2	Found with known V_s
		Ion part of the probe characteristic	
T_e^i (eV)	3.6	1.4	Assumes a Maxwellian EEDF
		(c) OML theory for electrons	
n_{OML}^i (cm^{-3})	1.1×10^{10}	9.6×10^{9}	Needs no knowledge of T_e
		(d) OML theory for ions	
$I_i(T_e^i)/I_{\text{exp}}$	180 μA/29 μA	9.4 μA/13 μA	$\eta=-eV_p/T_e=20$
$I_i(T_{\text{eff}})/I_{\text{exp}}$	15 μA/9 μA	36 μA/20 μA	λ_D was found from EEDF
a/λ_D	0.7	0.25	collisional sheath at p=0.3 Torr
		(e) Allen, Boyd, Reynolds, Chen theory	
n_{KP}^i (cm^{-3})	1.8×10^{9}	2.9×10^{9}	$V_p=-30$ V
n_{KP}^0 (cm^{-3})	4.1×10^{9}	1.8×10^{9}	Collisional sheath at p=0.3 Torr
b/a	13	13	
b/λ_i	0.58	5.8 (e) Kagan and Perel theory	

Torr) is 2.5 times less than that from the EEDF whereas using the true value of T_{eff}, n_{KP}^0 is just 7% less than that from the EEDF. Application of KP theory for p=0.3 Torr (where this theory is invalid) using T_e^i gives n_{KP}^i equal to that from the EEDF while using T_{eff} gives n_{KP}^0 that is 60% less than that from the EEDF.

VI. CONCLUSION

The result of determining the plasma parameters from the various procedures discussed here is summarized in Table I. As expected a departure of the EEDF from Maxwellian most strongly affects the electron temperature values when it is found from the probe characteristic in the neighborhood of the floating potential. This applies to any type of the floating probe measurement, i.e., the ion part of a single probe characteristic, as well as, double and triple probe techniques. When plasma density is inferred from ion current, the plasma potential V_p must be known since $V_p=V-V_s$. V_s is usually found from the measured floating potential V_f and the voltage across the sheath of the floating probe ΔV_f which can be calculated only for a known EEDF, otherwise the use of T_e^i and T_{eff} for calculation of ΔV_f is incorrect.

As shown by Vasileva[16,17] the shape of the EEDF affects the potential distribution around the probe and hence influences the current of attracted particles. Particularly, it has been shown[16,17] that the Debye length and ion current density in the Bohm-like expression for ion current are governed by the so-called screening temperature T_{es} but not by T_{eff}, such that $I_i\propto T_{es}^{1/2}$ and $\lambda_D\propto T_{es}^{1/2}$. The screening temperature T_{es} is determined as follows:

$$T_{es}=2\left(\int_0^\infty \epsilon^{-1/2}f(\epsilon)d\epsilon\right)^{-1}\neq T_{\text{eff}}=\frac{2}{3}\int_0^\infty \epsilon^{3/2}f(\epsilon)d\epsilon$$

and for a bi-Maxwellian EEDF as found here for 0.03 Torr

$$T_{es}=n[n_c/T_{ec}+n_h/T_{eh}]^{-1}\approx T_{ec}.$$

Thus, as seen in these formulas, the ion flux to the probe and the Debye length are governed by the low-energy part of the EEDF while the "floating" voltage ΔV_f and the electron temperature T_e^i (found from the ion part of the probe characteristic) is controlled by the high-energy part of the EEDF. These conclusions are consistent with experimental results given in Table I for plasma parameters inferred from the ion part of the probe characteristic. Note also that the true value λ_D should be determined through integration of the EEDF. For 0.03 Torr the true value of λ_D is determined by T_c since, within an accuracy of 1%, $T_{es}=T_{ec}$.

As for plasma parameters obtained using the classical Langmuir procedure, these are in reasonable agreement with those found from EEDF for the case of 0.03 Torr where the majority of electrons obey a Maxwellian distribution. Nonetheless, the temperature of the low-energy electrons found from a semilog plot of $I_e(V)$ is 50% larger than that found from $I_e''(V)$. For a Druyvesteyn-like distribution ($p=0.3$ Torr) there is a fundamental problem in finding the slope of $\ln I_e(V)$. The small linear part of $\ln I_e(V)$ in Fig. 4 appears to be irrelevant to the effective electron temperature and generates erroneous values for plasma parameters when used in calculations. An additional problem with a Druyvesteyn-like EEDF is the uncertainty in finding the plasma potential since there is no knee in the semilog plot of the probe characteristic measured with a thin probe. Druyvesteyn-like EEDF's are typical at relatively high gas pressure where the probe size limitations ($a \ll \lambda_e$) require the use of a very small probe. The plasma potential can confidently be found in the zero crossing point of the second derivative of the probe characteristic: $I''(V)=0$. But if one differentiates the probe characteristic, i.e., knows the EEDF, then there is no need of using the Langmuir procedure based on an assumption of a Maxwellian EEDF.

The shape of the electron part of the probe characteristics for $f(\epsilon) \propto \exp(-\epsilon/\alpha)^k$, where α and k are constants, has been analyzed by Vasileva[16] and Ershov *et al.*[18] They showed that the slope of $d \ln I_e(V)/dV$ in the energy interval about the mean electron energy $\langle\epsilon\rangle = 3/2\ T_{\text{eff}}$, adjacent to the plasma potential gives an electron temperature which is not too far from T_{eff}; but some independent method of finding the plasma potential is still needed to practically implement this idea.

Application of the traditional techniques for processing probe characteristics obtained in nonequilibrium plasma may lead to a significant error (up to 2–5 times) in defining the basic plasma parameters. The worst case occurs when inferring the electron temperature and plasma density from the ion part of the probe characteristic (also in double and triple probes) where the inferred value of T_e represents only the small portion of electrons which are in the high-energy tail of the EEDF. Unless there is a strong influence of electron-electron interaction, the energy distribution in the tail of the EEDF differs from that of the main body where the EEDF is close to Maxwellian. The departure from a Maxwellian distribution for high-energy electrons is most common in low-pressure gas discharges used in practical applications. The degree of departure of the EEDF from Maxwellian in a particular discharge and hence the error introduced in determining the plasma parameters from a probe diagnostic is not known in advance. Therefore, measurement of total probe characteristic followed by differentiation to get the EEDF is the most certain and reliable way to use probe diagnostics.

[1] V. A. Godyak, R. B. Piejak, and B. M. Alexandrovich, Plasma Sources Sci. Technol. **1**, 36 (1992).
[2] V. A. Godyak and R. B. Piejak, Phys. Rev. Lett. **65**, 996 (1990).
[3] I. Langmuir and H. Mott-Smith, General Electric Rev. **27**, 449 (1924).
[4] W. Verweij, thesis, University of Utrecht, 1960.
[5] J. G. Laframboise, Report No 100, University of Toronto, Institute of Aerospace Studies, 1966.
[6] I. B. Bernstein and I. N. Rabinowitz, Phys. Fluids **2**, 212 (1959).
[7] P. M. Chung, L. Talbot, and K. J. Touryan, *Electric Probes in Stationary and Flowing Plasmas: Theory and Application* (Springer, Berlin, Heidelberg, New York, 1975).
[8] A. von Engel, *Ionized Gases* (Clarendon, Oxford, 1955).
[9] D. Smith and I. C. Plumb, J. Phys. D **6**, 196 (1973).
[10] A. A. Sonin, AIAA **4**, 1588 (1966).
[11] C. H. Shih and E. Levi, AIAA **9**, 1673 (1971).
[12] B. M. Annaratone, M. W. Allen, and J. E. Allen, J. Phys. D **25**, 417 (1992).
[13] J. E. Allen, R. L. F. Boyd, and P. Reynolds, Proc. Phys. Soc. B **70**, 297 (1957).
[14] F. Chen, Plasma Phys., J. Nucl. Energy Part C **7**, 147 (1965).
[15] Yu. M. Kagan and V. I. Perel, Usp, Fiz. Nauk. **81**, 409 (1963) [Sov. Phys. Usp. **6**, 767 (1964)].
[16] I. A. Vasileva, Teplofiz. Vys. Temp. **12**, 29 (1974) (in Russian).
[17] I. A. Vasileva, Teplofiz. Vys. Temp. **12**, 473 (1974) (in Russian).
[18] A. P. Ershov, V. A. Dovzhenko, A. A. Kuzovnikov, and S. N. Oks, Fiz. Plasmy **7**, 609 (1981) [Sov. J. Plasma Phys. **7**, 334 (1981)].